

Supplementary Materials: Metamaterial Behavior of Polypropylene/Multi-Walled Carbon Nanotubes Fabricated by Means of Ultrasound-Assisted Extrusion

Juan C. Pérez-Medina, Miguel A. Waldo-Mendoza, Víctor J. Cruz-Delgado, Zoe V. Quiñones-Jurado, Pablo González-Morones, Ronald F. Ziolo, Juan G. Martínez-Colunga, Florentino Soriano-Corral and Carlos A. Avila-Orta

Four different fabrication methods were used to fabricate the polymer nanocomposites: W-U (without ultrasound), F-U (fixed-frequency ultrasound-assist fabrication), V-U (variable-frequency ultrasound-assist fabrication), and PT (pretreatment of MWCNT in a fluidized air-bed with an ultrasound probe).

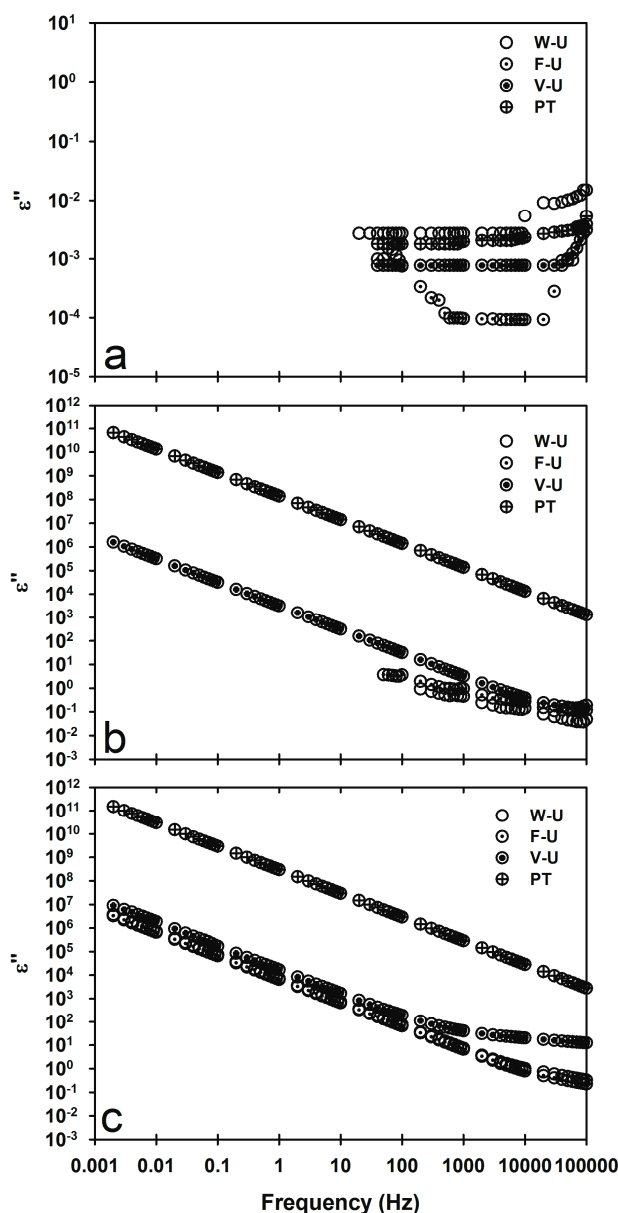


Figure S1. ϵ'' for (a) $iPP_{MFI=2.5}/MWCNT$; (b) $iPP_{MFI=34}/MWCNT$; and (c) $iPP_{MFI=1200}/MWCNT$ fabricated using different ultrasound-assisted extrusion methods.

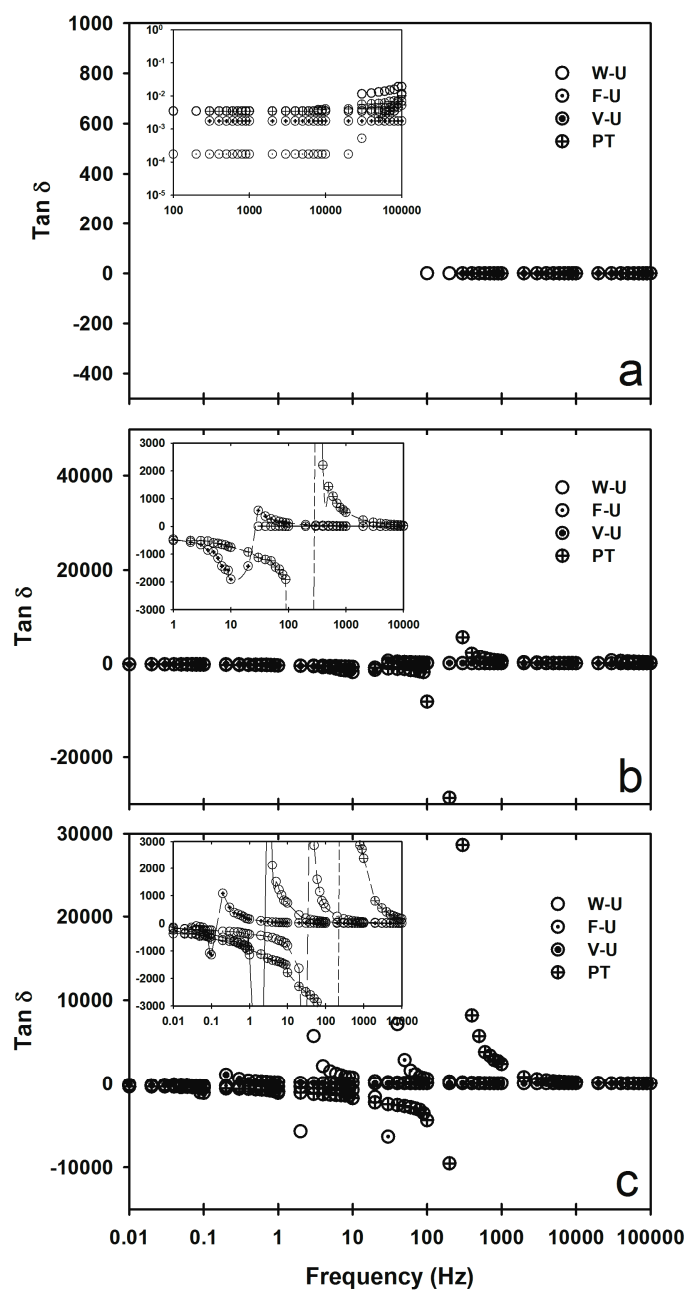


Figure S2. $\tan \delta$ for (a) $iPP_{MFI=2.5}/MWCNT$; (b) $iPP_{MFI=34}/MWCNT$; and (c) $iPP_{MFI=1200}/MWCNT$ fabricated using different ultrasound-assisted extrusion methods.

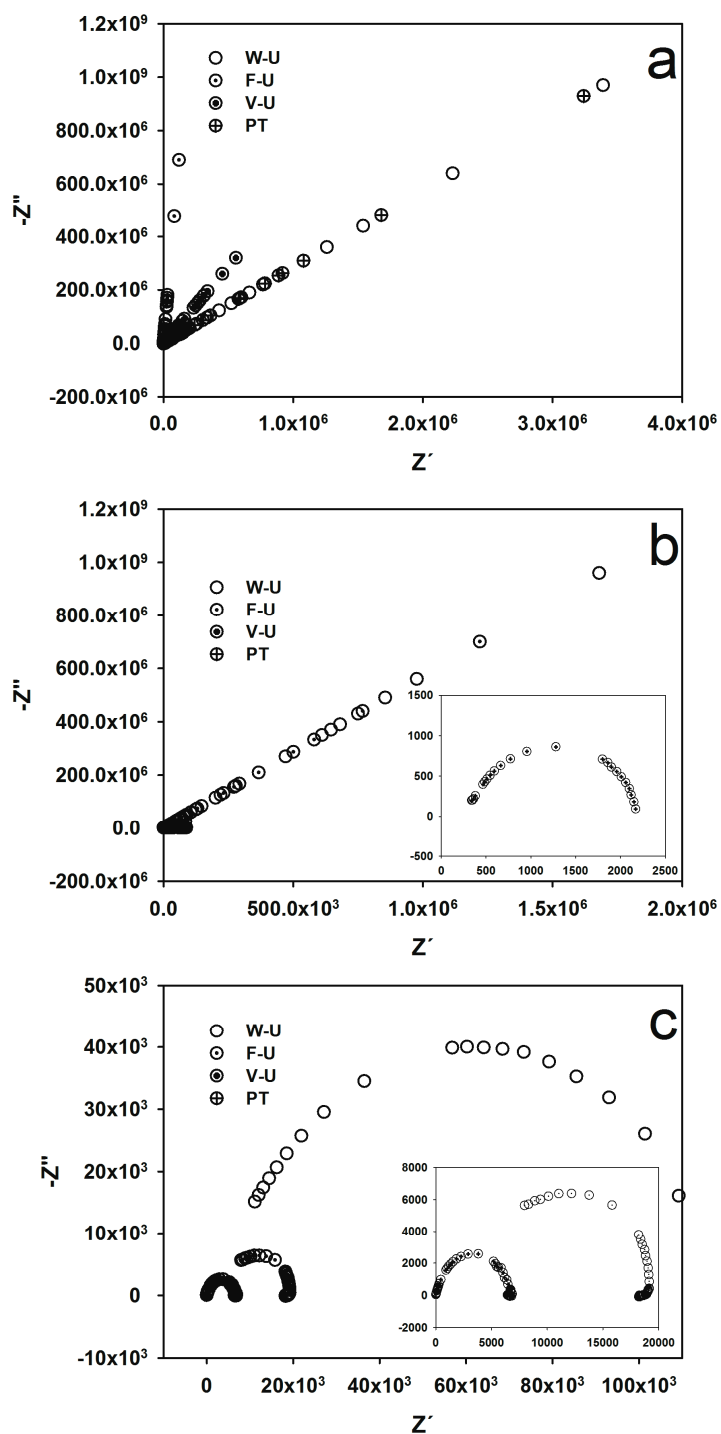


Figure S3. Nyquist plots for (a) $iPP_{MFI=2.5}/MWCNT$; (b) $iPP_{MFI=34}/MWCNT$; and (c) $iPP_{MFI=1200}/MWCNT$ fabricated using different ultrasound-assisted extrusion methods.

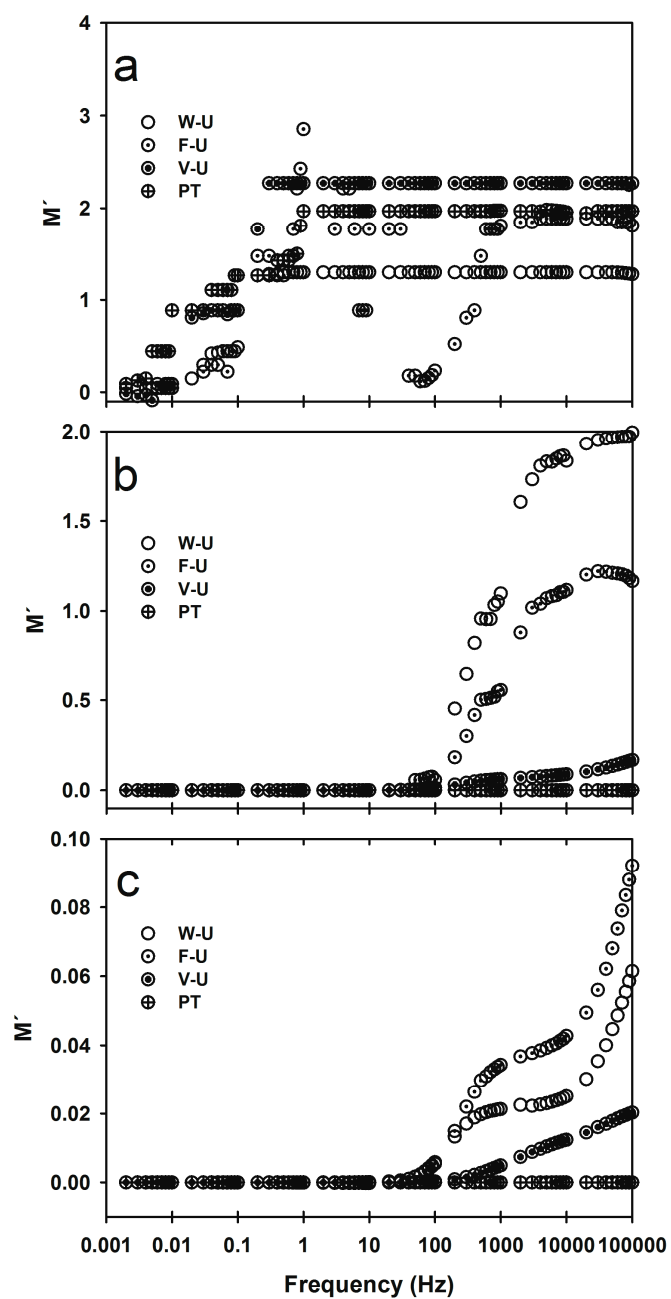


Figure S4. M' for (a) $iPP_{MFI=2.5}/MWCNT$; (b) $iPP_{MFI=34}/MWCNT$; and (c) $iPP_{MFI=1200}/MWCNT$ fabricated using different ultrasound-assisted extrusion methods.

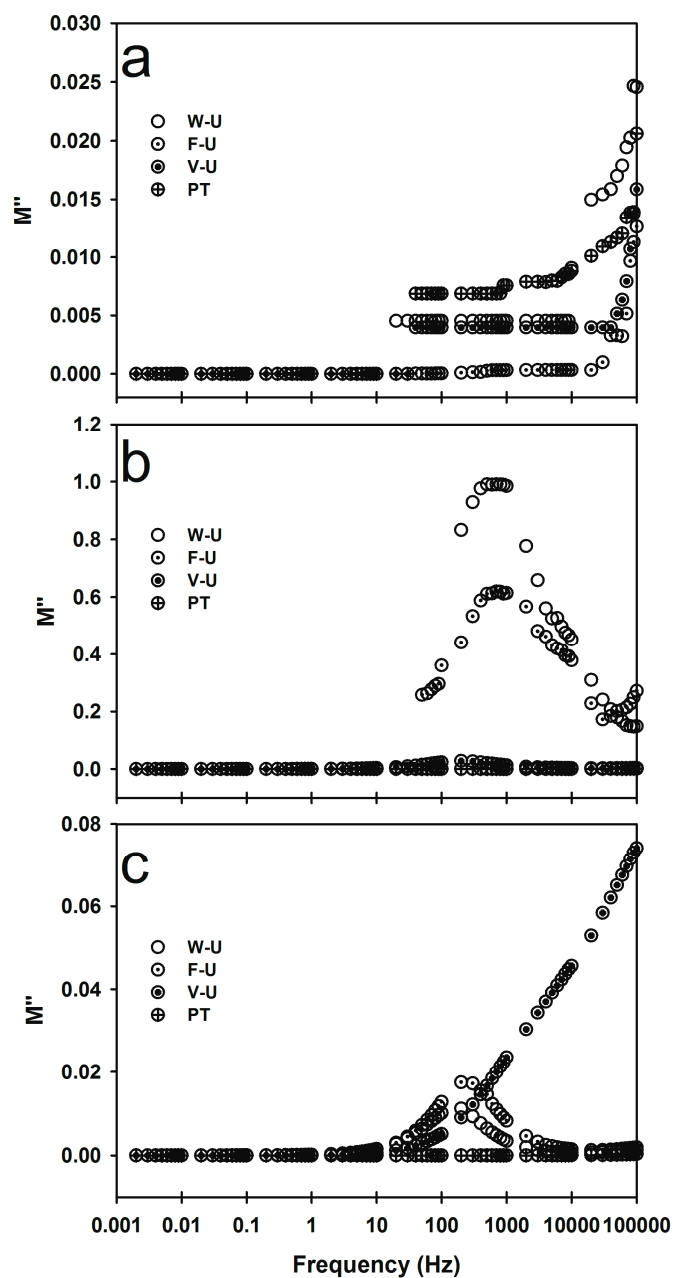


Figure S5. M'' for (a) iPP_{MFI=2.5}/MWCNT; (b) iPP_{MFI=34}/MWCNT; and (c) iPP_{MFI=1200}/MWCNT fabricated using different ultrasound-assisted extrusion methods.

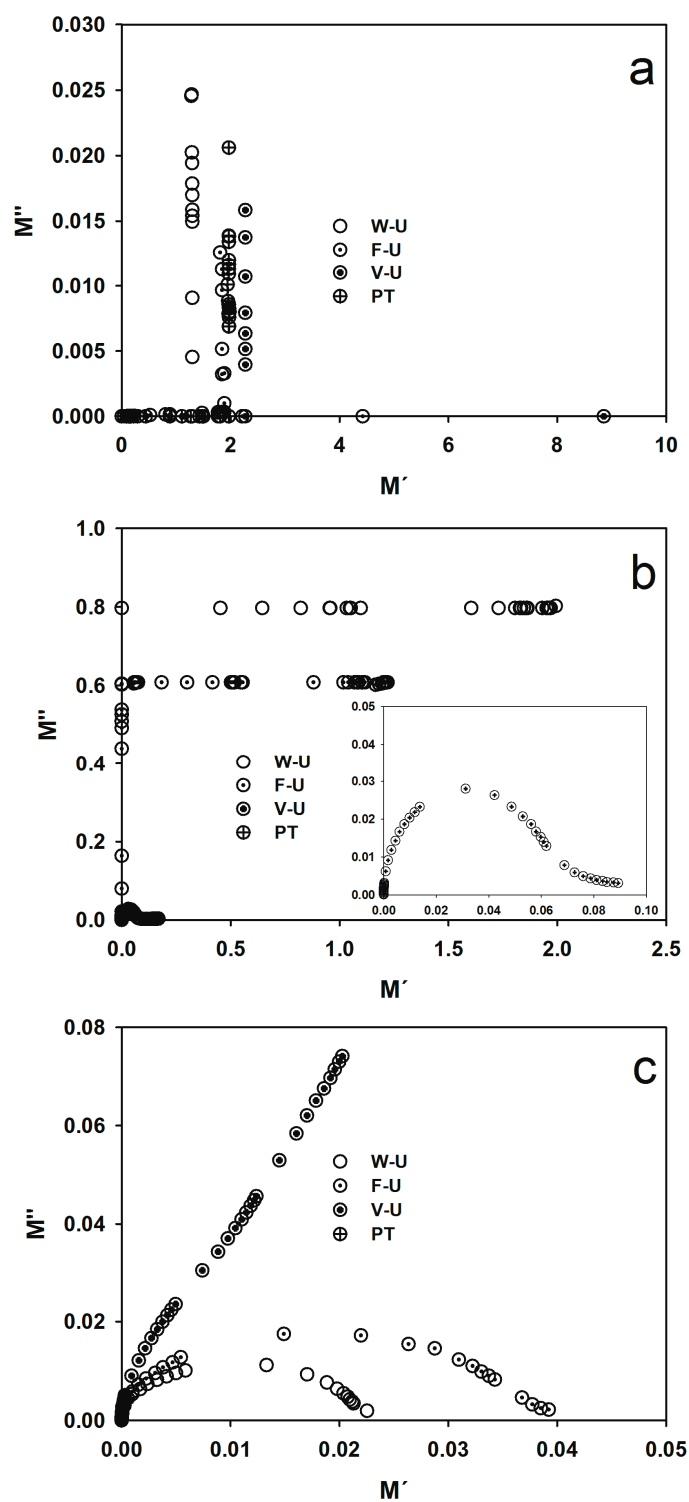


Figure S6. Electrical modulus complex plane (M'' vs. M') for (a) $iPP_{MFI=2.5}/MWCNT$; (b) $iPP_{MFI=34}/MWCNT$; and (c) $iPP_{MFI=1200}/MWCNT$ fabricated using different ultrasound-assisted extrusion methods.

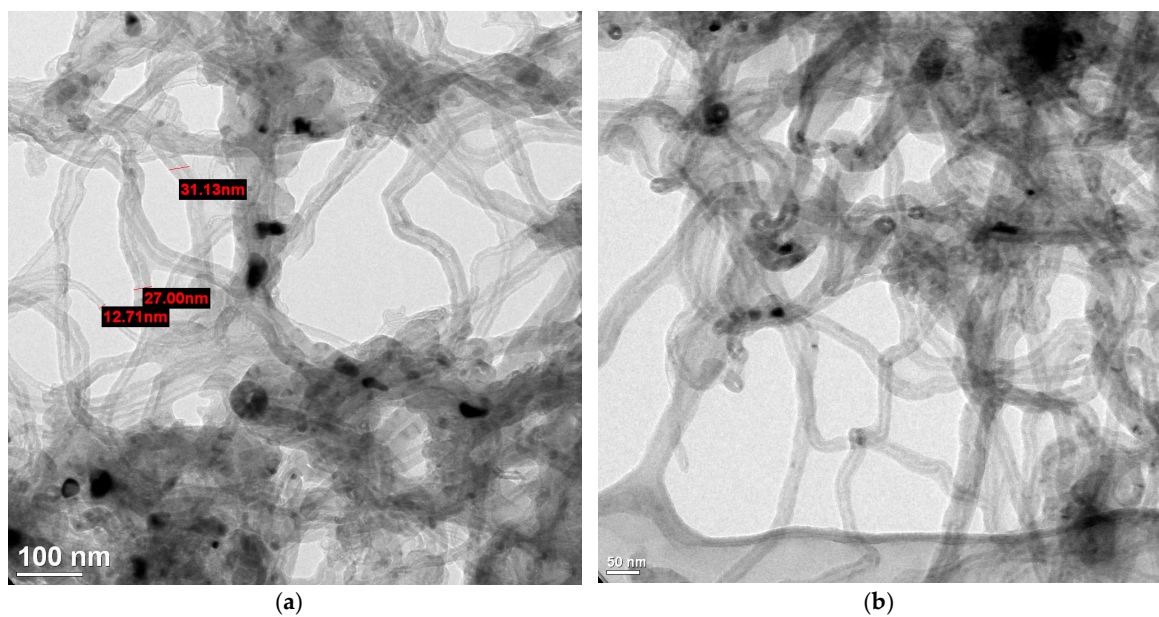


Figure S7. TEM micrographs of MWCNTs. (a) Lower magnifications; (b) Higher magnifications.